排灌机械工程学报
Journal of Drainage and Irrigation Machinery Engineering
2016 年 2 月 Feb. 2016 | 第 34 卷 第 2 期 Vol. 34 No. 2

Doi: 10.3969/j. issn.1674 -8530.15.0120

Computational fluid dynamics of left ventricular assist device under unsteady flow


BUMRUNGPETCH J.

BUMRUNGPETCH J.[1], *TAN A. C.*[2]

(1. Faculty of Science and Engineering, Queensland University of Technology, Brisbane QLD 4001, Australia;
2. LKC Faculty of Engineering and Science, University of Tunku Abdul Rahman, Bandar Sungai Long, Selongor 43000, Malaysia)

Abstract: Left ventricular assist device (LVAD) in this study is a mechanical tool that is used to support blood flow in the patient with heart disease. It supports left ventricle by building up the pressure to the pump outlet connected to the aorta. This pump was designed based on the magnetic driven centrifugal pump with a unique small washout hole constructed inside the impeller to generate the washout flow passage to prevent the stagnation at the region underneath and around the rotor. Computational fluid dynamics (CFD) was adopted in this study to assess the performance and optimize the design to avoid recirculation and high shear stress which is the main cause of stagnation and blood damage. Transient simulation was used for this study due to the asymmetric design of the washout hole and the complication of the bottom support of the impeller that has a risk of thrombosis, also, it was used to predict the variation of hydraulic performance caused by the rotation of the impeller and pulsed flow at the pump inlet. The simulation results show no excessive stress and no recirculation observed within the computational domain; in addition, the research result also provides information for further optimization and development to the pump.

Key words: heart pump; left ventricular assist device; computational fluid dynamics; unsteady flow
CLC Number: S277 **Document Code**: A **Article No**: 1674 -8530(2016)02 -0093 -06

Citation: BUMRUNGPETCH J, TAN A C. Computational fluid dynamics of left ventricular assist device under unsteady flow[J]. Journal of drainage and irrigation machinery engineering(JDIME), 2016,34(2):93 -98.

1 Introduction

Ventricular assist device (VAD) is a mechanical tool that is used to support blood flow in the patients with heart disease. It is now more increasingly used as it can be used for both bridge to transplant and long-term support until the heart function is recovered[1-2]. One of the major concerns regarding to the design of most centrifugal VAD is the area underneath the impeller where the blood could flow in and keep recirculating in the area, which could lead to thrombosis if the washout mechanic is not properly developed. The design of left ventricular assist device (LVAD) in this study provides a small hole inside the impeller to prevent this problem and the computational fluid dynamic (CFD) was employed for further analysis to identify the risk of thrombosis and predict the performance of the pump.

CFD analysis has been used as a tool for heart

Received date: 2015 -06 -08; **Publish time on line**: 2016 -01 -25
Online Publishing: http://www.cnki.net/kcms/detail/32.1814.TH.20160125.1104.020.html
Author information: BUMRUNGPETCH J. (1983—), male, bachelor of mechanical engineering(Jeerasit.Bumrungpetch@hrd.edu.au), researching in turbomachinery, numerical simulation.
TAN A. C. (1951—), male, Ph. D, professor(a.tan@qut.edu.au), researching in turbomachinery, numerical simulation.

pump development for several years[3-4], and several researchers have successfully simulated the heart pump flow and analysis using quasi-steady analysis in good agreement with the experimental results without considering the variation of flow rate[5-8]. For example, SONG et al[5] explores a quantitative evaluation of blood damage that occurs in a continuous flow left ventricular assist device due to fluid stress, and proved CFD was an effective approach to analyze Lagranian behavior of blood in a heart assist device. However, the design of the LVAD in this study contains several unbalanced and small structures that have a risk of forming recirculation flow and stagnation especially when it operates under the unsteady flow, where it would be the nature of operating condition for most blood bumps as the inlet of the device has to be connected to the ventricle that generates the pulsed flow when it contracts. Therefore, the evaluation needs to be carefully conducted and thus the transient simulation was adopted for this simulation as it could provide insight information for the unsteady flow rate condition [9-10].

2 Model and methodology

2.1 LVAD design

The LVAD pump used in this study is based on a small magnetic drive centrifugal pump which was designed to generate head pressure higher than 1.36 m at the rotation speed 2 900 r/min under the flow rate of 0.5 L/min to supply blood to the aorta, as seen in Fig. 1.

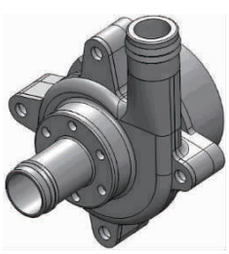

Fig. 1 3D model of LVAD

The pump comprises one inlet diameter 16.20 mm connected to the chamber directly to the eye of the impeller, and an outlet port diameter 13.50 mm, the impeller with 6 blade semi-open type impeller is suspended within the housing chamber by means of pivot bearing at the top and six small fin-shaped feet support the bottom of impellers. Inside the impeller, a through hole diameter 2.0 mm was constructed to create the flow passage from the bottom of the impeller that helps to remove recirculation which is the main cause of thrombosis within the pump, as seen in Fig. 2.

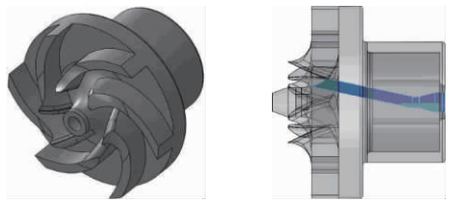

Fig. 2 Impeller model and structure of washout hole inside impeller

2.2 Simulation models and method

1) CFD model

The fluid model of the pump was constructed in Solidworks 2011, and the model was made into 2 separate parts, the stationary and the rotating domain. The stationary domain comprises inlet pipe, volute housing and the outlet pipe and the rotating domain represents the fluid volume around the impeller. The computational grid was generated in Ansys ICEM CFD meshing using the unstructured tetrahedral mesh method. The number of elements on the impeller and the housing approximate 412 000 and 909 000 respectively.

The grid independent test was conducted on the pump model to ensure that the current number of mesh was sufficient to convey the accurate results. The test was done by varying element density on the pump model and the steady state simulation was conducted for the result comparison. The number of mesh varied from estimated 80 000 to 2 500 000 elements with the approximate element ratio of stator to rotor 2∶1 and total 6 conditions were conducted.

The relation between the number of elements and the head pressure is shown in Fig. 3, where H is pump head, N is number of elements. It can be observed that the head pressures of the models comprise total 660 000 elements and tend to be steady. Consequently, it is verified that the current number of elements is sufficient for this study.

The working fluid in this simulation was set to re-

present the property of human blood with the density of 1 056 kg/m^3. The high shear stress within the pump makes the Newtonian behavior assumption of the blood viable [11] and thus the viscosity was set to be constant at 0.004 Pa · s.

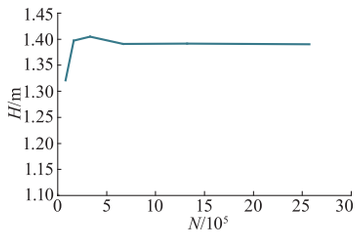

Fig. 3　Number of elements versus pump head

2) Turbulence model

The type of flow within the LVAD was predicted by the Reynolds number (Re) from the following equation:

$$Re = \frac{\rho \omega D^2}{\mu}, \quad (1)$$

where ρ is the fluid density, ω is the angular speed of the impeller, D represents the outer diameter of the impeller, and μ expresses the viscosity. An estimated Reynolds number of this LVAD was greater than 100 000 which means there is turbulence flow within the pump[11]. The turbulence model which was used to describe this characteristic of the flow is the standard $k-\varepsilon$ model.

3) Boundary conditions

There are three transient simulations conditions conducted in this study. The first condition has a variable flow rate at the inlet pipe of the pump to simulate the pulse flow from left ventricle; the second condition carries out the steady flow rate at the pump inlet but has smaller time step setting to exam the variation to the flow due to the impeller blades movement, and finally the last condition is the combination of the first and the second condition.

Condition Ⅰ: The input boundary of this condition is set to variable flow rate to replicate the pulse flow from left ventricle. The flow rate is based on the SONG's equation[11] for the left ventricle volumetric flow rate (Q) which is derived from the experimental data using a discrete Fourier transform as follows:

$$Q = C + \sum_{i=1}^{N} a_i \cos(2i\pi t) + b_i \sin(2i\pi t), \quad (2)$$

where $C = 5.430$, $a_1 = -0.485$, $a_2 = -0.143$, $a_3 = 0.267$, $b_1 = 1.589$, $b_2 = -0.095$, $b_3 = 0.097$ at the heart rate 60 bit/min.

The flow rate to the pump varies between 3.69 L/min and 7.48 L/min over 1 second period of time as shown in Fig. 4. The boundary condition for the outlet of the pump was set to static pressure 14.7 kPa. The time step for this simulation was set to 0.006 9 seconds, and 145 time steps were specified for 1 heart cycle. The result was obtained from the second beat in order to obtain the steady results.

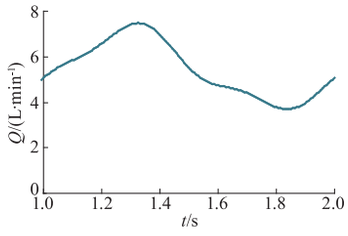

Fig. 4　Variable flow rate at the inlet of the pump in Condition I

Condition Ⅱ: The uniform constant flow rate of 0.5 L/min was applied to the inlet of this condition. In order to depict the effect of blades on the pump flow, smaller time steps are required, hence the time step was set to 0.000 517 5 s per step or 3° of impeller rotation per a time step. In order to obtain the steady results, the calculations were carried out for five revolutions of impeller or 0.310 5 s (600 time steps).

Condition Ⅲ: This condition has the pulse flow applied at the inlet while small time steps were also applied to capture the effect of impeller blade and washout hole to the hydrodynamic performance of the pump. The input boundary was pulsed flow as specified in Condition I and the outlet condition is static pressure 14.7 kPa. The time step size is 0.000 517 5 s but total period of time becomes 2 s or 2 heart cycles which means totally 3 800 time steps were calculated.

For all conditions, transient rotor/stator conditions with frozen rotor were applied, and the steady state simulation results of the nominal pump operating condition were used as an initializing condition to reduce the convergence time and computational resource for the simulation.

2.3　Hemolysis modeling

The blood damage estimation of this device is

done on the steady state condition based on the shear stress information generated within the device using the Eulerian method proposed by GARON and FARINAS[12]. This estimation method is done by integrating the linearized damage function of the red blood cell ($\overline{D}_{\mathrm{I}}$) and integrated over the whole domain as presented below.

$$\overline{D}_{\mathrm{I}} = \frac{1}{Q}\int_V \sigma \mathrm{d}V, \tag{3}$$

where Q is the flow rate, V is the volume of the device, σ is shear stress, and ($\overline{D}_{\mathrm{I}}$) is the average linear damage calculated from the relation:

$$D = (\overline{D}_{\mathrm{I}})^{0.785}. \tag{4}$$

From the damage value D, the normalized index of hemolysis (NIH) can be calculated by the following equations:

$$NIH = 100HbD. \tag{5}$$

3 Result and discussion

Condition Ⅰ: Head pressure of the pump is represented in Fig. 5. In this pump design the small drop on the flow rate at the inlet could cause large head pressure drop on the pump and thus there is a large variation on the overall pressure profile. The head pressure ranged from 1.35 m to 1.42 m under this simulated heart pulse.

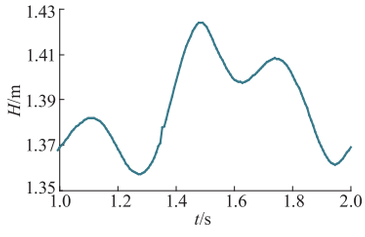

Fig. 5 Pump head under variable inlet flow

In addition to the head pressure, the pump structure that requires magnetic suspension to control the radial position of the impeller, the direction of total radial force (F_{r}) which is an accumulated force between F_x and F_y was identified by the following equation:

$$\theta = \tan^{-1}\frac{F_y}{F_x}. \tag{6}$$

Fig. 6 displays the radial force and the force trajectory in the polar coordinate during one heart cycle. The variation of force exerted on the impeller presented in this figure is a result of an asymmetry design of the pump volute. The magnitude of radial force is greater as the blood flow rate into the pump is increased, where it approximately ranged from 0.15 N to 0.50 N. This radial force exerted on the impeller is in the approximate direction between 310 – 330 N which is the direction of the wider side of the volute.

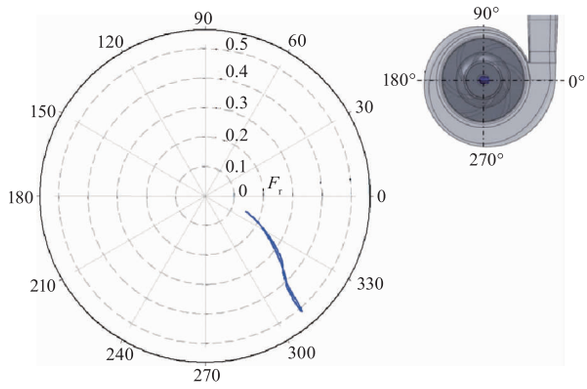

Fig. 6 Radial force trajectory on the impeller during one heart cycle

Condition Ⅱ: With the steady flow at the inlet and a smaller time step setting, the graphs between head pressure and radial force versus time are plotted in Fig. 7 and Fig. 8.

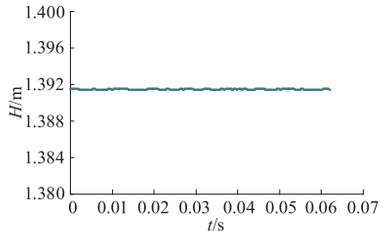

Fig. 7 Head pressure during one revolution of the impeller

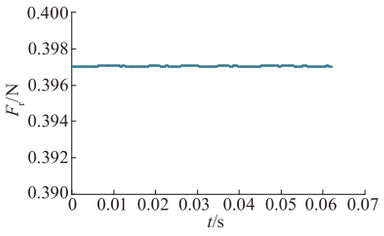

Fig. 8 Radial force during one revolution of the impeller

According to the graphs, the impeller blades and the out-flow from washout hole cause very small fluctuation that is almost unnoticeable on the head pressure of the pump and the radial force. The average head pressure approximates 1.39 m and the force pressure is estimated at 0.397 N in the same estimated direction as Condition I.

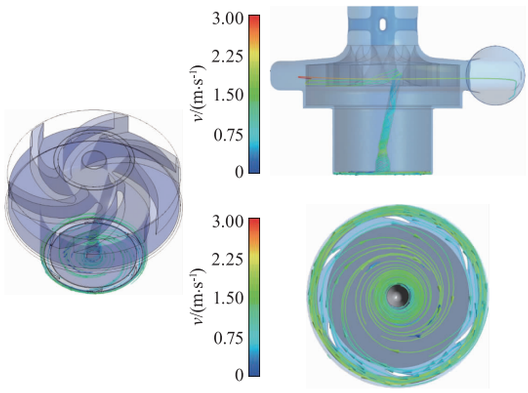

Fig. 9　Streamlines plotting of blood flow through the washout hole

Streamlines plotting in Fig. 9 displays the flow pattern of blood flow under the impeller through the washout hole. From the bottom view of the impeller, blood swirls in the same direction of the impellor rotation toward the washout hole at the middle; the flow velocity increases as it flows closer to the centre. The blood continues swirling through the washout hole as seen in the side view before becoming more uniform near the outlet at the top of the impeller then exit through the impeller vane. The flow rate through this washout hole is almost steady at 0.096 L/min or approximates 2% of the pump flow despite the unbalanced structure of the hole.

In order to identify the risk of stagnation within the washout hole, the velocity contour has been plotted on the cross-sectional plane during one revolution of the impeller, where the washout hole rotates to different positions as shown in Fig. 10. The low velocity region which indicates high chance of stagnation was not found in the washout hole at any impeller position.

Condition Ⅲ: A simulation of pulsed inlet flow with small time steps was conducted. The head pressure represented in Fig. 11 still presents the same trend as shown in Condition I, however, the fluctuation of the flow caused by impeller blades is higher than the variation found under the steady flow rate of Condition II. Therefore, further investigations were conducted at the time step 0.230 s where it has a high risk of thrombosis due to high fluctuation and low head pressure. The cross-section view of velocity contour at this time step is then plotted in Fig. 12, and there is no stagnation observed within the hole.

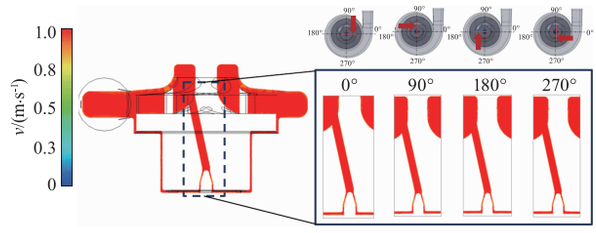

Fig. 10　Section view of velocity contour within the washout hole during one impeller revolution

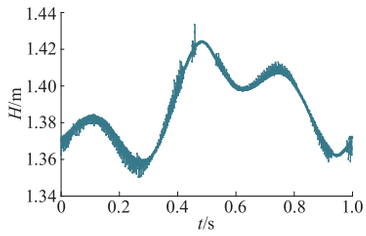

Fig. 11　Head pressure of the pump under Condition Ⅲ

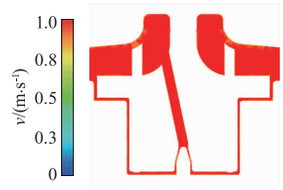

Fig. 12　Velocity contour in the washout hole at the time 0.230 s where high flow variation occurred in the pump

Despite higher fluctuation of the flow, variation in magnitude of the radial force exerted on the impeller is not significantly increased. The radial force is still in the range between 0.15 N and 0.51 N as shown in the polar coordinate plot in Fig. 13. However, this simulation can capture the fluctuation of force direction caused by the outflow from the washout hole which deviated around 15 N from the normal radial force profile previously observed in Fig. 6. This fluctuation of force occurred as the washout hole moved close to the volute tongue. The outflow was strong enough to cause the reaction force that disrupts the direction of normal radial force. It is notable that this force was not captured in Condition I which has larger time step and is not possible to be observed by the steady state simulation.

Blood damage estimation: The shear stress induced hemolysis generated from this LVAD was identified by the *NIH* index. According to the shear stress information from the steady state result the estimated *NIH* value of this device is 0.006 9 g/100 L.

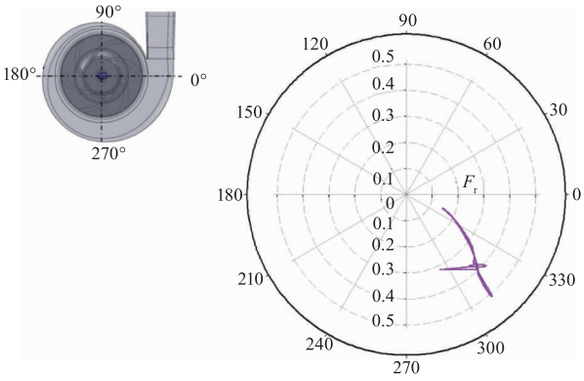

Fig. 13 Radial force trajectory on the impeller during one heart cycle of Condition Ⅲ

4 Conclusion

Although the steady state simulation could provide accurate results for the output performance and flow characteristic within the blood pump, the results from this study show that variation of the input flow from the ventricle pulse could amplify the fluctuation of the flow within the device. Therefore, transient simulation is the solid option for the analysis of the device which has complicated structures as it could provide greater details and more accurate results under different flow variations.

According to the simulation of all cases, the blood pump in this study could provide sufficient hydrodynamic performance to function as LVAD while the washout hole could perform efficiently in preventing the stagnation without having much negative impact on the overall pump performance. However, the experiment on the prototype under the pulse flow in the mock circulation loop is still a requirement for design verification as the next step for the future development.

References

[1] FIANE A E. Long-term left ventricle assist device (LVAD) therapy with rotary pumps[J]. Scandinavian cardiovascular journal, 2009,43(6):357 – 359.

[2] NOSÉ YUKIHIKO. Design and development strategy for the rotary blood pump[J]. Artificial organs, 1998, 22(6):438 – 446.

[3] BEHBAHANI M, BEHR M, HORMES M, et al. A review of computational fluid dynamics analysis of blood pumps[J]. European journal of applied mathematics, 2009, 20(3):363 – 397.

[4] MAY – NEWMAN K. Computational fluid dynamics models of ventricular assist devices[M]. Springer, 2010:297 – 316.

[5] SONG X, THROCKMORTON A L, WOOD H G, et al. Computational fluid dynamics prediction of blood damage in a centrifugal pump.[J]. Artificial organs, 2003, 27(10):938 – 941.

[6] FRASER K H, TASKIN M E, GRIFFITH B P, et al. The use of computational fluid dynamics in the development of ventricular assist devices[J]. Medical engineering & physics, 2010, 33(3):263 – 80.

[7] APEL J, NEUDEL F, REUL H. Computational fluid dynamics and experimental validation of a microaxial blood pump[J]. Asaio journal, 2001, 47(5):552 – 558.

[8] DAY S W, MCDANIEL J C, WOOD H G, et al. A prototype heartquest ventricular assist device for particle image velocimetry measurements[J]. Artificial organs, 2002, 26(11):1002 – 1005.

[9] BURGREEN G W, LOREE H M, BOURQUEK, et al. Computational fluid dynamics analysis of a maglev centrifugal left ventricular assist device[J]. Artificial organs, 2004,28:874 – 880.

[10] MAJIDI K. Numerical study of unsteady flow in a centrifugal pump[J]. Journal of turbomachinery, 2005, 127(2):805 – 814.

[11] SONG X, THROCKMORTON A L, WOOD H G, et al. Transient and quasi-steady computational fluid dynamics study of a left ventricular assist device[J]. Asaio journal, 2004, 50(5):410 – 417.

[12] GARON A, FARINAS M I. Fast three-dimensional numerical hemolysis approximation[J]. Artificial organs, 2004, 28(11):1016 – 1025.

(责任编辑 盛杰)